Medical Engineering & Physics 32 (2010) 679–689

Contents lists available at ScienceDirect

Medical Engineering & Physics

journal homepage: www.elsevier.com/locate/medengphy

Review

Application of higher order statistics/spectra in biomedical signals—A review

Kuang Chua Chua[a,*], Vinod Chandran[b], U. Rajendra Acharya[a], Choo Min Lim[a]

[a] Department of Electronics and Computer Engineering, Ngee Ann Polytechnic, 535 Clementi Road, Singapore 599489, Singapore
[b] Queensland University of Technology, Australia

ARTICLE INFO

Article history:
Received 6 May 2009
Received in revised form 8 April 2010
Accepted 10 April 2010

Keywords:
Higher order spectra
Spectrum
Electrocardiogram
Heart rate variability
Electroencephalogram
Epilepsy
Entropy
Linearity
Stationary
Gaussianity
Bispectrum
Bicoherence

ABSTRACT

For many decades correlation and power spectrum have been primary tools for digital signal processing applications in the biomedical area. The information contained in the power spectrum is essentially that of the autocorrelation sequence; which is sufficient for complete statistical descriptions of Gaussian signals of known means. However, there are practical situations where one needs to look beyond autocorrelation of a signal to extract information regarding deviation from Gaussianity and the presence of phase relations. Higher order spectra, also known as polyspectra, are spectral representations of higher order statistics, i.e. moments and cumulants of third order and beyond. HOS (higher order statistics or higher order spectra) can detect deviations from linearity, stationarity or Gaussianity in the signal. Most of the biomedical signals are non-linear, non-stationary and non-Gaussian in nature and therefore it can be more advantageous to analyze them with HOS compared to the use of second-order correlations and power spectra. In this paper we have discussed the application of HOS for different bio-signals. HOS methods of analysis are explained using a typical heart rate variability (HRV) signal and applications to other signals are reviewed.

Contents

1. Introduction

HOS techniques were first applied to real signal processing problems in 1970s, and since then they have continued to expand into different fields such as economics, speech, seismic data processing,

* Corresponding author. Tel.: +65 64606896; fax: +65 64671730.
E-mail address: ckc@np.edu.sg (K.C. Chua).

1350-4533/$ – see front matter © 2010 IPEM. Published by Elsevier Ltd. All rights reserved.
doi:10.1016/j.medengphy.2010.04.009

plasma physics, optics and biomedicine. The estimation of power spectrum of discrete-time deterministic or stochastic signals is one of the most fundamental and useful tools in digital signal processing. The use of power spectrum spreads across radar, sonar, communication, speech, biomedical, geophysical, and other data processing systems. In power spectral estimation, the signal under consideration is processed in such a way that the phase relationship among components is lost. The information contained in the power spectrum is essentially that which is present in the autocorrelation sequence and is sufficient to describe a Gaussian signal completely. HOS offers some unique features that make it more advantageous for use in some applications. Some of the motivations behind the use of higher order spectra in signal processing are as follows:

(i) HOS of non-Gaussian linear processes contains both amplitude and phase information. They have been used for time-series modeling, and identification of non-minimum phase and non-causal systems. These applications include signal reconstruction from speckle images, seismic deconvolution and channel equalization.
(ii) The HOS of Gaussian signals are statistically zero. Thus, HOS can be used to measure non-Gaussianity and to separate additive mixtures of independent non-Gaussian signals and Gaussian noise. This feature can be exploited to detect and classify non-Gaussian signals and provide high noise immunity in application where the signal source is corrupted with Gaussian noise.
(iii) A general non-linear system can be modeled using an nth-order Volterra processor [1]. HOS is able to detect and characterize the non-linear properties of mechanisms which generate time series via phase relations of their harmonic components.
(iv) HOS are translation invariant because linear phase terms are cancelled in the products of Fourier coefficients that define them. Functions that can serve as features for pattern recognition can be defined from higher order spectra that satisfy other desirable invariance properties such as scaling, amplification, and rotation invariance.

HOS have been applied to many applications such as in oceanography [2], 1D pattern recognition [3,4], chaotic signal characterization [5], array signal processing [6], telecommunication [7], ultrasound image processing [8], 2D pattern recognition [9] detection of mines from sonar images [10], study of machine faults [11], recognition of viruses from electron microscopic images [12], termite detection [13], analysis of bio-signals like the ECG [14] and the EEG [15].

Many aspects of healthcare require the processing and analysis of physiological signals such as electroencephalogram (EEG), electrocardiogram (ECG), heart rate variability (HRV), electromyogram (EMG) and medical images. This may require tasks such as noise reduction, feature extraction/detection, pattern analysis/classification, visualization and modeling. Some of the inherent characteristics of biomedical signals are non-linearity, non-stationarity, non-Gaussianity, uncertainty and imprecision.

Bio-signals are essentially non-stationary signals; they often display a fractal like self-similarity. They may contain indicators of current disease, or even warnings about impending diseases. The indicators may be present at all times or may occur at random—in the time scale. However, to (study and) pinpoint anomalies in voluminous data collected over several hours is strenuous and time consuming. Therefore, a robust analytical tool for in-depth study and classification of data collected over long intervals can be very useful in diagnostics. The use of non-linear features motivated by the higher order spectra (HOS) has been reported to be a promising approach to analyze the non-linear characteristics of the bio-signals. These HOS-based non-linear dynamical techniques are based on chaos theory and have been applied to many areas including the areas of medicine and biology. The basic principles of HOS are discussed in Section 1. Different HOS techniques are used to analyze the data are discussed in Sections 2 and 3. Section 4 of the paper covers the application of HOS to various bio-signals. Section 5 provides a discussion and the paper concludes in Section 6.

2. HOS and features derived from HOS

2.1. Higher order spectra

Higher order spectra are defined to be spectral representations of higher order cumulants of a random process.

Let $x(k)$ be a real, discrete time and nth-order stationary random process. Moreover, let $w = [w_1, w_2, \ldots w_n]^T$ and $x = [x(k), x(k+\tau_1), \ldots, x(k+\tau_{n-1})]^T$. Then the nth-order moment of $x(k)$, $m_n^x(\tau_1, \tau_2, \ldots, \tau_{n-1})$ is defined as the coefficient in the Taylor expansion of the moment generating function

$$\phi(w) = E[\exp(iw^T x)] \tag{1}$$

In practice, the nth-order moment can be equivalently calculated by taking an expectation over the process multiplied by $(n-1)$ lagged versions of itself [16]

$$\begin{aligned} m_1^x &= E[x(k)] \\ m_2^x &= E[x(k)x(k+\tau)] \\ m_3^x &= E[x(k)x(k+\tau_1)x(k+\tau_2)] \\ m_4^x &= E[x(k)x(k+\tau_1)x(k+\tau_2)x(k+\tau_3)] \end{aligned} \tag{2}$$

Similarly, the coefficients in the Taylor expansion of the cumulant generating function, also known as the second characteristic function

$$x(w) = \ln E[\exp(jw^T x)] \tag{3}$$

are nth-order cumulants of $x(k)$ denoted by $c_n^x(\tau_1, \tau_2, \ldots, \tau_{n-1})$.

Combining (1) and (3) it is obvious that cumulants can be expressed in terms of moments and vice versa. One can easily calculate cumulants as certain non-linear combinations of moments. The second-, third- and fourth-order cumulants are [17,18]

$$\begin{aligned} c_1^x &= m_1^x \\ c_2^x(\tau) &= m_2^x(\tau) - (m_1^x)^2 \\ c_3^x(\tau_1, \tau_2) &= m_3^x(\tau_1, \tau_2) - m_1^x[m_2^x(\tau_1) + m_2^x(\tau_2) + m_2^x(\tau_2 - \tau_1)] + 2(m_1^x)^3 \\ c_4^x(\tau_1, \tau_2, \tau_3) &= m_4^x(\tau_1, \tau_2, \tau_3) - m_2^x(\tau_1)m_2^x(\tau_3 - \tau_2) - m_2^x(\tau_2)m_2^x(\tau_3 - \tau_1) \\ &\quad - m_2^x(\tau_3)m_2^x(\tau_2 - \tau_1) - m_1^x[m_3^x(\tau_2 - \tau_1, \tau_3 - \tau_1) \\ &\quad + m_3^x(\tau_2, \tau_3) + m_3^x(\tau_1, \tau_2)] + (m_1^x)^2[m_2^x(\tau_1) + m_2^x(\tau_2) + m_2^x(\tau_3) \\ &\quad + m_2^x(\tau_3 - \tau_1) + m_2^x(\tau_3 - \tau_2) + m_2^x(\tau_2 - \tau_1)] - 6(m_1^x)^4 \end{aligned} \tag{4}$$

If the signal $x(k)$ is zero mean $m_1^x = 0$, then the second- and third-order cumulant are identical to second- and third-order moments, respectively. If the process has nonzero mean, the mean may be subtracted from it first and this is often the practice with estimation from finite records. However, to generate the fourth-order cumulant we need to have the knowledge of the fourth-order and second-order moments, i.e.

$$\begin{aligned} c_4^x(\tau_1, \tau_2, \tau_3) = {} & m_4^x(\tau_1, \tau_2, \tau_3) - m_2^x(\tau_1)m_2^x(\tau_3 - \tau_2) \\ & - m_2^x(\tau_2)m_2^x(\tau_3 - \tau_1) - m_2^x(\tau_3)m_2^x(\tau_2 - \tau_1) \end{aligned} \tag{5}$$

In practice, because of unique linear property of the second characteristic function working with cumulants and cumulant spectra instead of moments is more common and preferable in the case of stochastic signals. However, it is noteworthy that estimates of cumulants are obtained in practice after computing estimates of moments from time-domain samples using their relationship. Besides, higher order spectra are often estimated directly in the

spectral domain as expected values of higher order periodograms. In cases where HOS are estimated in spectral domain, cumulants may not be calculated. Cumulant spectra can be obtained from moment spectra in the spectral domain through similar relationships [17–19].

Cumulants of the first three orders at zero lag are the well known parameters, variance, skewness and kurtosis used to describe probability density functions.

By putting $\tau_1 = \tau_2 = \tau_3$ into the equations above, we obtain

$$\gamma_2 = E\{x_2(k)\} = c_2^x(0) \quad \text{(variance)} \tag{6}$$

$$\gamma_3 = E\{x_3(k)\} = c_3^x(0) \quad \text{(skewness)} \tag{7}$$

$$\gamma_4 = E\{x_4(k)\} - 3(\gamma_2)^2 = c_4^x(0,0,0) \quad \text{(kurtosis)} \tag{8}$$

The second, third and forth order cumulant are the variance, the skewness and kurtosis of the histogram of the time series, respectively. They describe the profile of the distribution, for example kurtosis can be used to measure 'peakedness' of the distribution of a series [20].

2.2. Frequency domain definition and properties

The second-order cumulant spectrum is the power spectrum and the, third-, and fourth-order cumulant spectra are known as the bispectrum and the trispectrum, respectively.

General formula

$$S_n^x(\omega_1, \omega_2, \ldots, \omega_{n-1}) = \sum_{\tau_1=-\infty}^{\infty} \cdots \sum_{\tau_{n-1}=-\infty}^{\infty} cum_n^x(\tau_1, \tau_2, \ldots, \tau_{n-1}) \exp\left[-j\sum_{i=1}^{n-1}\omega_i\tau_i\right] \tag{9}$$

When $n = 2$, we have power spectrum:

$$S_2^x(\omega) = \sum_{\tau=-\infty}^{\infty} cum_2^x(\tau)\exp[j\omega\tau] \tag{10}$$

Bispectrum: $n = 3$

The bispectrum is the 2D-Fourier transform of the third cumulant function:

$$S_3^x(\omega_1, \omega_2) = \sum_{\tau_1=-\infty}^{\infty}\sum_{\tau_2=-\infty}^{\infty} c_2^x(\tau_1, \tau_2)\exp[-j(\omega_1\tau_1 + \omega_2\tau_2)] \tag{11}$$

for $|\omega_1| \le \pi$, $|\omega_2| \le \pi$, and $|\omega_1 + \omega_2| \le \pi$.

In the above definitions, it is assumed that the moment or cumulant functions satisfy the conditions necessary for a Fourier (spectral) representation. This implies that they decay with increasing lags and are at least square integrable. For discussion on existence of polyspectra for random processes, refer to [17]. Note that the cumulants are deterministic functions even though the process is random.

For a deterministic signal $x(n)$, the power spectrum can be expressed in terms of the Fourier transform of the underlying signals as:

$$S_2(\omega) = X^*(\omega)X(\omega)$$

For a deterministic, zero-DC signal the bispectrum may be expressed in terms of the Fourier transform of the underlying signal since

$$S_3^x(\omega_1, \omega_2) = \sum_{\tau=-\infty}^{\infty}\sum_{\tau=-\infty}^{\infty}\sum_{n=-\infty}^{\infty} x(n)x(n+\tau_1)x(n+\tau_2) \times \exp[-j(\omega_1\tau_1 + \omega_2\tau_2)] \tag{12}$$

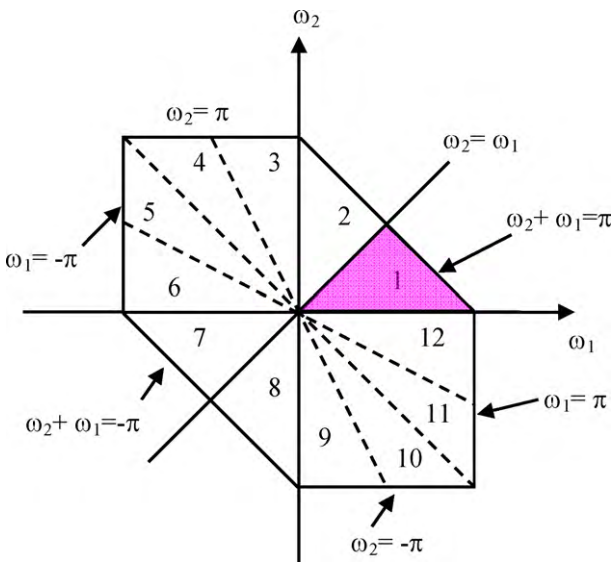

Fig. 1. Non-redundant region of computation of the bispectrum of a discrete-time signal assuming that the sampling interval is 1 and the Nyquist frequency is thus π rad/s.

setting $n + \tau_1 = m$ and $n + \tau_2 = k$ and splitting the exponent it can be shown that

$$S_3^x(\omega_1, \omega_2) = \left\{\sum_{m=-\infty}^{\infty} x(m)e^{-j\omega_1 m}\right\}\left\{\sum_{k=-\infty}^{\infty} x(k)e^{-j\omega_1 k}\right\} \times \left\{\sum_{n=-\infty}^{\infty} x(n)e^{+j(\omega_1+\omega_2)n}\right\} = X(\omega_1)X(\omega_2)X^*(\omega_1+\omega_2) \tag{13}$$

Note that in the expressions above for the power spectrum and the bispectrum of a deterministic signal, these spectra are products of Fourier transforms of the deterministic time-domain signals. The bispectrum is a triple product evaluated at two frequencies and their sum frequency. This expression is similar the periodogram expression for power spectrum and is referred to as a higher order periodogram. It can be shown that the bispectrum of a random process can be estimated as the expected value of this bi-periodogram over an ensemble of realizations of the process. Often only a single realization of the process is all that is available. If the process is indeed stationary, this realization can be divided into segments and bi-periodograms from the different segments can be averaged to obtain a reliable estimate of the bispectrum.

If $x(n)$ is a finite duration sequence the existence of its (discrete) Fourier transform (DFT) is guaranteed.

The symmetry conditions of the bispectrum $S_3(\omega_1, \omega_2)$ follow from those of the third cumulant, namely:

$$\begin{aligned} S_3(\omega_1, \omega_2) &= S_3(\omega_2, \omega_1) = S_3{}^*(-\omega_2, -\omega_1) = S_3{}^*(-\omega_1, -\omega_2) \\ &= S_3(-\omega_1 - \omega_2, \omega_2) = S_3(\omega_1, -\omega_1 - \omega_2) \\ &= S_3(-\omega_1 - \omega_2, \omega_1) = S_3(\omega_2, -\omega_1 - \omega_2) \end{aligned} \tag{14}$$

Thus, knowledge of the bispectrum in the triangular region $\omega_2 \ge 0$, $\omega_2 \ge \omega_1$, $\omega_1 + \omega_2 \le \pi$ is sufficient to describe the rest (Fig. 1). This region (labeled 1) is often termed the principal region or the non-redundant region of computation of the bispectrum.

The bispectrum is the spectral decomposition of skewness of the histogram of the time series, and the trispectrum is the spectral decomposition of the kurtosis of the histogram of the time series. Put another way, whenever the histogram of a time series is

skewed, the bispectrum must be different from zero. The reverse is not true, but if the time series is generated by a Gaussian process, the bispectrum is zero.

2.3. Estimation of higher order spectra

In practice, even if the underlying process is random and continuous, digital computations require discrete or sampled data and the data available are of finite length. Just like the power spectra, there are two main approaches that can be used to estimate higher order spectra [21]: the conventional non-parametric methods (or "Fourier type") and the parametric approach—i.e. based on autoregressive model (AR), moving average (MA), autoregressive and moving average (ARMA) or Volterra model. The interested reader may refer to tutorials in [18,21] for the details of these methods. The Matlab based Higher Order Spectral Analysis toolbox [22] consists of various functions to estimate HOS both in parametric and non-parametric methods, as well as some utility functions for various test and measurements.

The methodology adopted in the results presented here is the parametric approach. Simply put, the bi-periodogram as in Eq. (13) is computed for all available records in an ensemble or all segments obtained from a finite record. These segments may be made to overlap to improve statistical reliability. The bi-periodgram is averaged over the entire ensemble to obtain the estimate of the bispectrum.

3. Analysis using HOS features

3.1. Bispectrum, bicoherence and quadratic phase coupling

The estimate of the bispectrum of a stationary and ergodic random process with the non-parametric approach is given by

$$B(f_1, f_1) = E[X(f_1)X(f_2)X^*(f_1 + f_2)] \tag{15}$$

where $X(f)$ is the Fourier transform of a segment (or windowed portion) of a single realization of the random signal $x(nT)$, n is an integer index, T is the sampling interval and $E[.]$ stands for the expectation operation. Note that a finite length record of a single realization of the random process is a deterministic signal and it is absolutely summable in discrete form and its Fourier transform is guaranteed to exist. The expectation operation over a number of realizations is extremely important for statistical reliability. Windowing introduces spectral leakage in the DFT operation and provided this effect can be ignored, the bispectrum of the original random process can be expected to be close to the estimate computed by Eq. (15). Statistics of the bispectrum and effects of leakage are discussed in [23].

The bispectrum is a function of two frequencies unlike the power spectrum which is a function of one frequency variable. The frequency f may be normalized by the Nyquist frequency (one half of the sampling frequency) to be between 0 and 1. The bispectrum can be normalized (by power spectra at component frequencies) such that it has a magnitude between 0 and 1, and indicates the degree of phase coupling between frequency components [18,21].

Phase coupling occurs due to non-linear interactions between harmonic components. Three harmonics with frequencies f_k and phases ϕ_k, $k = 1, 2, 3$, are said to be quadratically phase coupled if $f_3 = f_1 + f_2$ and $\phi_3 = \phi_1 + \phi_2$. Quadratic phase coupling (coupling at sum and difference frequencies) occurs when a signal is passed through a square-law device, for example, and may be detected from the bispectrum. The magnitude of bispectrum may be affected by the signal by the strength of the signals as well as the phase relationship. Therefore the normalized form of bicoherence is commonly used to identify the quadratic phase coupling relationship.

A normalized bispectrum by Haubrich [24] is given by

$$B_{norm}(f_1, f_2) = \frac{E(X(f_1)X(f_2)X^*(f_1+f_2))}{\sqrt{P(f_1)P(f_2)P(f_1+f_2)}} \tag{16}$$

where $P(f)$ is the power spectrum. Bicoherence, $B_{co}(f_1, f_2)$, is defined as the squared-magnitude of the normalized bispectrum. If the Fourier components at the frequencies f_1, f_2 and $f_1 + f_2$ are perfectly phase coupled in every realization (or block of data) the bicoherence will be 1. If they are completely random-phase the bicoherence would be 0, in theory. Since the power spectral values in the denominator are estimates in practice, this normalization does not ensure that the magnitude of the normalized bispectrum obtained from finite time series will be bounded by 1. An alternative normalization of the bispectrum by Kim and Powers [25] ensures that the magnitude of the normalized bispectrum will be bounded by 1, as has been proved using the Schwartz inequality. Kim and Powers bicoherence is given by

$$B_{norm}(f_1, f_2) = \frac{E[(X(f_1)X(f_2)X^*(f_1+f_2))]}{\sqrt{E[P(f_1)P(f_2)]E[P(f_1+f_2)]}} \tag{17}$$

This is important only if we are interested in measuring the degree of phase coupling between frequency components reliably. In practice when we have only an estimate of the bispectrum or the bicoherence from a finite number of realizations, the estimate has a finite bias and variance. Values of bicoherence [26] and tricoherence [21] at various significance levels are known for Gaussian random noise. It is known that the bicoherence and tricoherence are asymptotically Chi-squared distributed [21,26]. If N realizations are averaged to compute the estimate, 95% of the bicoherence values should lie between 0 and $6/2N$. Thus, if 100 independent blocks of data are averaged in the estimate, a bicoherence greater than 0.03 would be significant at the 95% confidence level to reject the hypothesis that the particular frequency components came from a Gaussian noise process. The case of a harmonic random process is discussed in [21]. For other processes, values for the random-phase hypothesis at different significance levels can be determined by randomizing the phases of the Fourier components while keeping the magnitude (and hence the power) spectrum the same and computing the distribution of bicoherence values. If the data blocks are short, the statistics of the bispectrum and the bicoherence can also be influenced by spectral leakage [3]. Bicoherence plots of zero mean and unit variance Gaussian noise and generalized extreme value noise with 100 blocks of data and each block 256 samples are shown in Fig. 2.

The bicoherence of Gaussian random variable is nearly zero with about 5% of the distribution above the 95% significance level of 0.03 as expected. For generalized extreme value random variable, the bicoherence is not statistically 0. It is found in the experiment above that about 13% of the bicoherence distribution over the triangular region of computation lies above the 95% significant level. It can therefore be concluded that the bicoherence is not zero at the 95% level of confidence for this distribution. Hinich [27] has developed statistical tests for Gaussianity and test for linearity based on HOS.

Fig. 3 shows a sample of real bio-signal which is a typical heart rate signal of a normal subject.

Fig. 4 shows the bispectrum and its normalized version, the bicoherence, for the HRV signal shown in Fig. 3.

The heart rate we resampled using algorithm in [28], and the sampled data were partition into blocks of 512 points with an overlap of 256 points (i.e. 50%). The bicoherence were computed from the average value of 11 blocks of data altogether giving the value of 95% confident level of 0.2727 (i.e. $b_{95\%} = 6/2N = 6/22$).

The bispectrum plot can be used to examine the non-linear interaction between harmonic components of a signal. For *normal* HRV signal (shown in Fig. 3), the bispectrum magnitude plot exhibits peaks at lower frequencies (Fig. 4(a)). The heart rate is varying continuously between 60 and 80 beats per minute (bpm). The

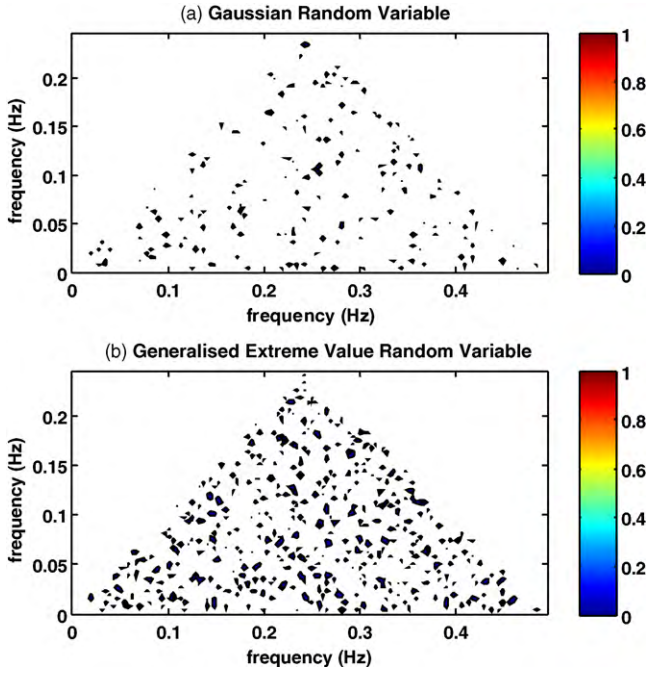

Fig. 2. Bicoherence noise plots: (a) Gaussian and (b) generalized extreme value noise with 100 blocks of data and each block 256 samples.

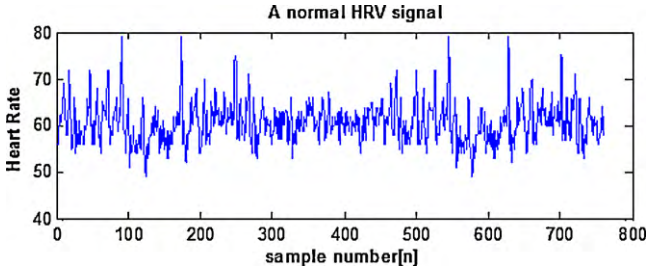

Fig. 3. Typical heart rate signal of normal subject.

bicoherence plot is shown in Fig. 4(b). Bicoherence values appear to be scattered through out the bifrequency plane in a random manner.

3.2. Other derived features from bispectrum

Besides testing for linearity, detecting quadratic phase coupling and checking for Gaussianity, HOS will provide information about

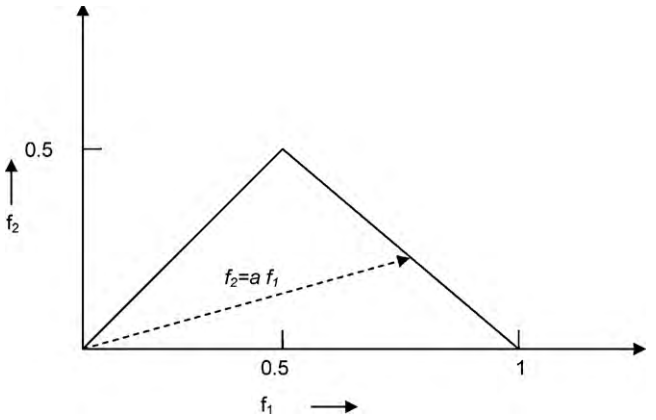

Fig. 5. Region of computation of the bispectrum for real signals. Features are calculated by integrating the bispectrum along the dashed line with slope = a. Frequencies are shown normalized by the Nyquist frequency.

signal wave shape. Assuming that there is no bispectral aliasing, the bispectrum of a real signal is uniquely defined with the triangle $0 \le f_2 \le f_1 \le f_1 + f_2 \le 1$. Parameters are obtained by integrating along the straight lines passing through the origin in bifrequency space [4]. The region of computation and the line of integration are depicted in Fig. 5. The bispectral invariant, $P(a)$, is the phase of the integrated bispectrum along the radial line with the slope equal to a. This is defined by

$$P(a) = \arctan\left(\frac{I_i(a)}{I_r(a)}\right) \tag{18}$$

where

$$I(a) = \int_{f_1=0^+}^{1/(1+a)} B(f_1, af_1)df_1 = I_r(a) + jI_i(a) \tag{19}$$

for $0 < a \le 1$, and $j = \sqrt{-1}$. The variables I_r and I_i refer to the real and imaginary part of the integrated bispectrum, respectively.

These bispectral invariants contain information about the shape of the waveform within the window and are invariant to shift and amplification and robust to time-scale changes. These features are rotation, translation and scaling invariant when applied to one- and two-dimensional pattern recognition [4,9]. They are particularly sensitive to changes in the left–right asymmetry of the waveform. For windowed segments of a white Gaussian random process, these features will tend to be distributed symmetrically and uniformly about zero in the interval $[-\pi, +\pi]$. If the process is chaotic and exhibits a coloured spectrum with third order time correlations or phase coupling between Fourier components, the mean value and

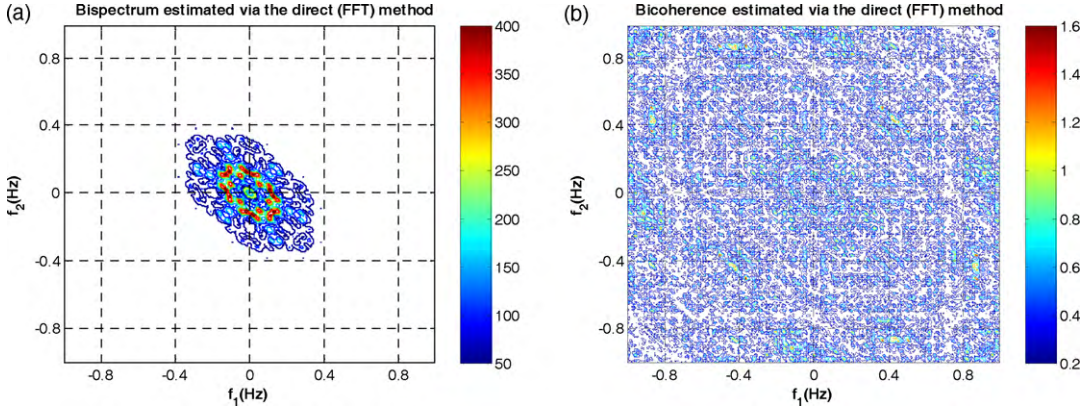

Fig. 4. Plots of (a) bispectrum and (b) bicoherence of Fig. 3.

the distribution of the invariant feature may be used to identify the process.

Ng et al. [29] have used mean magnitude and phase entropy as features to investigate images in particular on photomontage. We present these features here. However, unlike their work, we calculated these features within the region 1 defined in Fig. 1 (which is equivalent to Ω of Fig. 5):

$$\text{Mean magnitude of the bispectrum}: \quad M_{\text{ave}} = \frac{1}{L}\sum_{\Omega} \left|b(f_1, f_2)\right| \tag{20}$$

$$\text{Phase entropy}: \quad P_e = \sum_n p(\psi_n)\log p(\psi_n) \tag{21}$$

$$p(\psi_n) = \frac{1}{L}\sum_{\Omega} 1(\phi(b(f_1, f_2)) \in \psi_n) \tag{22}$$

$$\psi_n = \left\{\phi \left| -\pi + \frac{2\pi n}{N} \le \phi < -\pi + \frac{2\pi(n+1)}{N}\right.\right\}, \quad n = 0, 1, \ldots, N-1 \tag{23}$$

where L is the number of points within the region in Fig. 5, ϕ refers to the phase angle of the bispectrum, Ω refers to the space of the defined region in Fig. 1, and 1(.) is an indicator function which gives a value of 1 when the phase angle ϕ is within the range of bin ψ_n in Eq. (23).

In bio-signal processing, bispectrum plots are derived from different classes of signals and found to be different in structure and distribution of values. There have been several attempts to define features to distinguish these plots. These features are derived from the centroid, moments or the entropies of the distributions.

The weighted center of bispectrum (WCOB) [30] is given by

$$f_{1m} = \frac{\sum_{\Omega} iB(i,j)}{\sum_{\Omega} B(i,j)} \qquad f_{2m} = \frac{\sum_{\Omega} jB(i,j)}{\sum_{\Omega} B(i,j)} \tag{24}$$

where i and j are the frequency bin index in the non-redundant region.

Entropies were used to characterize the regularity or irregularity of the bio-signals from bispectrum plots. Chua et al. [31] have defined two bispectral entropies similar to that of spectral entropy [32]. The formulae for these bispectral entropies are given as:Normalized bispectral entropy (BE 1):

$$P_1 = -\sum_n p_i \log p_i \tag{25}$$

where

$$p_i = \frac{\left|B(f_1, f_2)\right|}{\sum_{\Omega}\left|B(f_1, f_2)\right|} \tag{26}$$

Ω = the region as in Fig. 5.Normalized bispectral squared entropy (BE 2):

$$P_2 = -\sum_n p_n \log p_n \tag{27}$$

where

$$p_n = \frac{\left|B(f_1, f_2)\right|^2}{\sum_{\Omega}\left|B(f_1, f_2)\right|^2} \tag{28}$$

Ω = the region as in Fig. 5.

The normalization in the equations above ensures that entropy is calculated for a parameter that lies between 0 and 1 (as required of a probability) and hence the entropies (P_1 and P_2) computed are also between 0 and 1.

The features related to moments [33] the plot are:

The sum of logarithmic amplitudes of the bispectrum:

$$H_1 = \sum_{\Omega} \log(|B(f_1, f_2)|) \tag{29}$$

The sum of logarithmic amplitudes of diagonal elements in the bispectrum:

$$H_2 = \sum_{\Omega} \log(|B(f_k, f_k)|) \tag{30}$$

The first-order spectral moment of amplitudes of diagonal elements in the bispectrum:

$$H_3 = \sum_{k=1}^{N} k \log(|B(f_k, f_k)|) \tag{31}$$

Although in this paper, all these features are defined within the principle domain in figure, one could also compute these features based on bispectrum of all the quadrants. An example of normal HRV signal with its corresponding bispectrum and bicoherence is given below:

P_1=0.6911, P_2=0.4698, P_e=3.5713, M_{ave}=1.82e05
H_1=6.04e04, H_2=567, H_3 = 3.08e4,
f_{1m} = 25.29 and f_{2m} = 8.848.

$P(a)$ = 1.0518, $P(a)$ = −2.1798 for a = 1/16 and 3/16, respectively are values for Fig. 5.

In many biomedical application, HOS (mainly bispectrum or bocoherence) analysis were performed on the signal of interest. Often the plot of the bispectrum or bicoherence enables us to differentiate different physiological states or pathological conditions. However, it is difficult to make use of the plots for automatic recognition by computers. These derived features discussed in this section are parameters proposed by various researchers to facilitate automatic machine learning.

4. Application of HOS on various signals

The HOS has been used to analyze various different bio-signals namely electroencephalogram (EEG), electrocardiogram (ECG)/heart rate (HR) signals, electromyogram (EMG), lung sounds, heart sounds, bowel sounds and medical images. They are briefly explained below.

4.1. Electroencephalogram (EEG) analysis

Probably one of the most popular application of HOS in biomedical fields is in the study of EEG [34–44]. Researchers have found dependence of individual frequency components in a signal for the EEG during defined physiological states such as sleep or anesthesia. Thus, the use of higher order spectral analysis capable of detecting interrelations between individual signal components has proved useful [35]. At different level of anesthesia for example, the quadratic phase coupling relations will be different.

The bispectrum and bicoherence index showed some prominent peaks at low-frequency components indicating the existence of QPC in [36]. This study also found that both the undisturbed (EEG) and the specifically activated states of the brain (auditory evoked potential) exhibit interactions between neuronal substrates oscillating in different frequencies. QPC in EEG from Alzeheimer's patients was studied in [40]. They found QPC in the evoked potential EEGs in the delta, theta, alpha and beta bands. Bicoherence was used to examine the deviation from Gaussianity and linearity, and QPC of the EEG of different mental states (eye-closing and eye-opening) in [41]. It was found that the eye-closed state was more non-linear and more non-Gaussian.

HOS features have been used to monitor the depth of anesthesia successfully [42]. They have presented a model that generalizes the autoregressive class of polyspectral models by having a semi-parametric description of the residual probability density. A bispectral index derived from bispectral analysis of EEG recordings was used to quantify the depth of anesthesia in [43].

HOS has also been used to characterize the dynamics of sleep spindles using sleep EEG signals [44]. Their results show that, the normalized spectrum and bispectrum, described frequency interactions associated with non-linearities occurring during sleep spindle EEG activity.

In order to facilitate machine learning, different researchers proposed different derived features as a mean of differentiating the bispectrum plots. These features are described in Section 3.2. Bispectral analysis was used for non-invasive detection of cerebral ischemia in rats [30]. The maximum magnitude and the weighted center of EEG bispectrum (WCOB) change according to the extent and the place of the injury region. The study indicated that the EEG bispectrum analysis may be useful to distinguish the ischemic region from the normal one and to estimate the extent of cerebral ischemia.

Bispectral features were used to classify EEG signals corresponding to left/right-hand motor imagery [33]. The feature set included parameters derived from moments of the power spectrum and moments based on the bispectrum of EEG signals. Experimental results have shown that based on the proposed features, the LDA classifier, SVM classifier and NN classifier achieved better classification results than those of the BCI-competition 2003 winner [45].

Huang et al. have developed an new approach, based on bispectrum analysis of EEGs and an artificial neural network (ANN), to predict seizures [46]. The maximum magnitude and the weighted center of EEG bispectrum (WCOB) were extracted from the EEG bispectrum contour and a four-layer ANN was used for prediction. The proposed system was able to correctly predict the succedent seizures and prediction times ranged from 12 to 24 s, prior to the onset of epileptic seizures.

Recently HOS-based measures such as bispectrum entropy and bispectrum phase entropy to distinguish normal, pre-ictal and seizure stages have been proposed in [47]. These entropy based features discriminate between the classes with high confidence levels (p-value of less than 0.05). Normal, pre-ictal and epileptic EEG classes were identified using HOS features with a classification accuracy of 93.11% in [48]. They have shown the superiority of the performance of HOS-based features as compared to the PSD features which yielded classification accuracy up to 88.78% for the three classes (normal, pre-ictal and epileptic) with the same classifiers.

4.2. ECG and HRV analysis

Third-order cumulant on 1-d slices and a four-layer neural network classifier was used to classify ECG late potentials in [49]. They were able to classify normal, confirmed, and suspected abnormal subjects with an accuracy of 96%.

The degree of changes in the dominant frequencies during ventricular fibrillation using Wigner transforms was studied on dogs by [50]. They have used auto-bispectra to quantify phase coupling between different dominant rhythms. Their results show that during ventricular fibrillation there is substantial frequency modulation of the dominant rhythms and these rhythms are phase coupled.

A new way of detecting the R-wave in a QRS complex of an electrocardiogram (ECG) based on higher order statistics (HOS) was presented by [51]. They used HOS-based parameters, such as skewness and kurtosis, to identify the R peak with an accuracy of 99%.

Atrial fibrillation (AF) and ventricular tachycardia (VT) are other types of tachy-arrhythmias that constitute a medical challenge. Ventricular fibrillation (VF) and ventricular tachycardia (VT) ECG parameters were derived by AR modeling using PSD as well as AR modeling using HOS in [52]. Classification results with Learning Vector Quantization (LVQ) code books demonstrated that HOS-based AR modeling performed better than the PSD based one in classifying VF and VT. An algorithm based on the bispectral analysis for the analysis and classification of cardiac arrhythmias was proposed by [14]. The bispectrum was estimated using an autoregressive model and it was observed that different arrhythmias occupied different range of f_1 and f_2 in the bispectrum plot. This frequency ranges called "frequency support" of the bispectrum was used to classify atrial and ventricular tachy-arrhythmias. Their study showed a significant difference in the parameter values for different arrhythmias.

The most difficult problem faced in automatic ECG analysis is large variation in the morphologies of ECG waveforms, not only of different patients or patient groups but also within the same patient. The ECG waveforms may differ for the same patient to such extend that they are unlike to each other and at the same time alike for different types of beats. As a result, the beat classifier which perform well on the training data may fare badly when presented with different patients ECG waveforms [53]. In their study, they show that the higher order statistics are less sensitive to the variation of morphology of ECG. Motivated by this, Engin developed a fuzzy-hybrid neural network for electrocardiogram (ECG) beat classification with features consisted of the combination of autoregressive model coefficients, higher order cumulant and wavelet transform variances instead of the original ECG beats [54]. In this approach wavelet tranforms captured non-stationary information and HOS characterized the non-Guassian information and reduced the variation due to morphological changes. Over all effect of combining different features for the classifier resulted a better performance of classification of 98% accuracy when tested on the MIT/BIH arrhytmia database [55]. In a saparate work, Oswoski et al. have developed an ECG recognition system using HOS features and the support vector machine (SVM) [53]. Their expert system was able to achieve an average error rate of less than 4% for the recognition of 13 heart rhythm types.

The compression performance and characteristics of two wavelet coding compression schemes of electrocardiogram (ECG) signals suitable for real-time telemedical applications was studied in [56]. The two proposed methods, namely the optimal zonal wavelet coding method and the wavelet transform higher order statistics-based coding method, were used to assess the ECG compression issues. HOS with wavelet analysis achieved high compression ratio with low compression error.

Chua et al. have proposed unique bispectrum and bicoherence plots for the normal and seven cardiac arrhythmia classes using the HRV signal [31]. HOS features such as bispectrum invariant features and bispectrum entropies derived for these cardiac states were found to be statistically significant (p-value <0.02). They have also classified cardiac states (normal and three abnormal) using HOS parameters with an average classifier efficiency of more than 85% [57].

The heart rate variability (HRV) can be taken as an indicator of the coordination of the cardio-respiratory rhythms. In [68] bispectral analysis shown that the occurrence of a quadratic phase coupling (QPC) between a low-frequency (LF: 0.1 Hz) and a high-frequency (HF: 0.4–0.6 Hz) component of the HRV during quiet sleep in healthy neonates.

4.3. Analysis of surface electromyogram (sEMG)

Researchers have reported that sEMG has shown non-Gaussian property [59,60]. This suggests that HOS could uncover additional information that second-order analysis could provide.

It is important for a quality neuromuscular diagnosis to obtain information on innervation pulse trains and motor-unit action potentials (MUAPs) characteristics. Non-linear decomposition based on HOS for the synthetic surface-EMG (sEMG) signals was studied reliably in a noiseless case in [61]. They also tested different levels of additive Gaussian noise and found out that the robustness of HOS to such noise leads to satisfactory results in noisy environments. The cepstrum of bispectrum based system reconstruction algorithm was applied to recover MUAP from wired-EMG (wEMG) and surface-EMG (sEMG) signals in the Rectus Femoris and Vastus Lateralis muscles in [62]. In this work MUAP estimates recovered from cepstrum of bispectrum were comparable in quality to those produced by the multiple electrode approach but without the need for specialized equipments. Furthermore, it was observed that the appearance of the estimated MUAPs clearly showed evidence of motor-unit recruitment and crosstalk, if any, due to activity in the neighbouring muscle.

Kaplanis et al. have used HOS to analyze the surface-EMG signal (sEMG) [63]. They have shown that the level of Gaussianity of sEMG changed as mean voluntary contraction (MVC) varied. The signal became less Gaussian at very low and very high MVC but some were at the middle, sEMG became more Gaussian. The level of non-Gaussianity of sEMG signal variation was used to classify sEMG signals [64]. They compared the performances of seven different combinations of cumulant-based feature vectors for sEMG classification. They used the Sequential Forward Selection (SFS) to select the best feature set in a high-dimensional feature set generated by the HOS. With only three selected features (i.e. $C_{2,x}(0)$, $C_{2,x}(1)$ and $C_{4,x}(0,0,0)$) they were able to achieve an average classification accuracy of 93.23%.

Recently Chen et al. [65] has proposed discriminant bispectrum (DBS) feature to classify the predefined hand and wrist motions, and compare it with several widely used first- and second-order features such as AR, PSD, RMS and time-domain (TD) statistics. Their experiment demonstrates that the DBS feature, containing non-Gaussian and non-linear information of the sEMG signal, is superior to those first- and second-order statistics for motion classification, and suggests that HOS has good potential for improving prosthetic control.

4.4. Analysis of other bio-signals—lung sound, heart sound, bowel sounds and somatosensory evoked potential

The QPC of the lung sound on preclassified signals (wheezes, ronchi, stridors) was studied [66]. They observed three distinguished peaks (410.2 Hz, 820.4 Hz, and 1230.6 Hz) in the power spectrum of inspiratory stridor, at f_0, $2f_0$ and $3f_0$, respectively. On the other hand, the corresponding bispectrum of the signal showed only a sharp peak in the bifrequency domain, located at $(f_1, f_2) = (410.2\,\text{Hz}, 410.2\,\text{Hz})$. This is an indication that a strong quadratic phase coupling among the frequencies of the related frequency pair and hence a non-linear production mechanism of respiratory stridors.

HOS was used in an autoregressive modeling to characterize the source and transmission of lung sounds [67]. The lung sound source in the airway was estimated using the prediction error of an all-pole filter based on higher order statistics (AR-HOS), while the acoustic transmission through the lung parenchyma and chest wall is modeled by the transfer function of the same AR-HOS filter. The study had showed a reliable and consistent estimation of lung sound characteristics for different lung diseases using HOS method, even in the presence of additive Gaussian noise.

An adaptive heart-noise reduction method, based on fourth-order statistics (FOS) of the recorded signal, without requiring recorded "noise-only" reference signal was presented in [68]. This algorithm was used to preserve the entire spectrum. Furthermore, the proposed filter was independent of Gaussian uncorrelated noise and insensitive to the step-size parameter.

A kurtosis (zero-lag fourth-order statistic) technique for the detection of non-stationary bioacoustic signals, such as explosive lung and bowel sounds, in clinical auscultative recordings was presented [69]. The iterative kurtosis-based detector (IKD) detected important peaks of the kurtosis, estimated within a sliding window along the signal under investigation, which indicated the presence of non-Gaussianity in the raw signal. Experimental results demonstrated IKD's ability to detect bioacoustic signals of diagnostic interest in the presence of background signal with high amplitude.

Studies conducted by different researchers showed that a phonocardiogram (PCG) is a non-Gaussian process [68,70]. They demonstrated different bispectral structures in both normal and pathological heart sounds. Hence, polyspectra may be an effective and useful tool for understanding the basic heart sound mechanism and improving diagnostic sensitivity via heart sounds.

Bispectrum is time-shift invariant and the initial phase of a signal cannot not be recovered. However, when studying of somatosensory evoked potential (SEP) signals this initial phase provides the major information, especially when it characterizes pathologies. Meste [71] derived a recursive algorithm that can extract some information of this signal phase. This method lead to details enhancement while preserved the latency estimation of the SEP signals.

4.5. Analysis of 2D bio-signals

A new method based on higher order statistics for detection of microcalcifications in mammograms was proposed in [72]. Mammogram images were first band-passed filter without subsampling. Microcalcifications gave rise to small isolated bright regions which forms outliers which modify the histogram of the image. The bandpass filtered sub-image was divided into overlapping square regions in which skewness and kurtosis were used as measures of the asymmetry and impulsiveness of the distribution. Their study showed that a region with high positive skewness and kurtosis was successfully used in detecting regions with microcalcifications.

Abeyratne and Petropulu have modeled a tissue as a collection of point scatterers embedded in a uniform media in [73]. They showed that the higher order statistics (HOS) of the scatterer spacing distribution can be estimated from digitized RF scan line segments and can be used to characterize tissue signatures.

Two-dimensional images have been transformed into one-dimensional signals for HOS analysis. This was done using Radon transform [9] or using slicing algorithm [74]. Features that were invariant to shift, scaling and rotation were used for pattern recognition and texture analysis. Invariant features based on HOS were used for virus recognition in [12]. Viral particles from one or more images were segmented and analyzed to verify whether they belong to a particular class (such as Adenovirus and Rotavirus) or not. Bispectral features and Gaussian mixture modeling of their probability density were shown to be effective in identifying viruses from electron microscope images. Another group of researchers also developed similar invariant features based on the phase of the bispectrum moment [75] and these features were used to automatically recognize and classify malignant lymphomas and leukemia [76].

Acharya et al. have automatically identified the normal, mild diabetic retinopathy (DR), moderate DR, severe DR and prolific DR using the bispectral invariant features of higher order spectra techniques and support vector machine (SVM) classifier in [77]. They have obtained an average accuracy of 82% in identifying the unknown class and sensitivity, specificity of 82% and 88%, respectively.

A computer-based intelligent system for the identification of *clinically significant* and *clinically non-significant* maculopathy fundus eye images was proposed in [78]. Bispectrum invariants and Sugeno fuzzy model based fuzzy classifier were used for the automatic identification. They demonstrated a sensitivity of 97% and specificity of 100% for the classifier and results are very promising.

5. Discussion

Time-domain measures of variability are easy to compute and provide valuable prognostic information about patients. They are susceptible to noise which causes baseline wander and artifacts. The time-domain and second-order methods may not always be able to identify different bio-signals (different rhythms) as these signals may have identical means and standard deviations. Hence, more rigorous techniques to differentiate these physiological signals are necessary to derive clinically useful information.

Fourier and wavelet transforms can be used to analyze the signal in the frequency domain. The signal is assumed to be implicitly periodic to apply the discrete Fourier transform. In the interpretation of experimental data, periodic behaviour may or may not exist when evaluating alterations in spectral power in response to intervention. The signal is also assumed to be stationary. The assumption of stationarity may not hold when the signal is recorded for long durations and when underlying mechanisms of signal generation change. Spectral analysis is more sensitive to the presence of artifacts than time-domain methods.

Wavelet transforms (WT) were found to be more suitable for the bio-signal analysis than the Short Time Fourier Transform (STFT) because of their better resolution. It is able to extract dynamical information from the signals. STFT and WT help to convey the frequency information at a particular instant. But they fail to extract non-linear relationships within the signal or time series.

Higher order spectral analysis can be used as a powerful tool for the non-linear dynamical analysis of the physiological signals. It was observed that HOS techniques would be a better approach than traditional time-domain and frequency domain methods in analyzing the bio-signals. It performs better when applied to weak and noisy signals.

Human body is a complex system that often exhibits some complex form of compensation or interaction. For example, there are several pacemakers in human heart. If certain part of heart is injured and the pacemaker at this region fail, others surrounding pacemaker will take over some of the load. As a result the rhythm of the heart pumping and heart rate will alter accordingly. This form of compensation could in some where lead to non-linear interaction and hence produce bio-signal that will have quadratic phase coupling. Although the process may not be well understood, experimental results indicated there are information that can be picked in QPC [57,58] and in the bispectral plots [31].

Likewise, EEGs are very complex signals with possible non-linearity interaction among its frequency components and perhaps some form of phase coupling. These "random" signals cannot be fully described by second-order measures. Our experiment shows that the classifier with HOS-based features outperformed the classifier with second-order measures (i.e. power spectrum). High-order statistic information was able to reveal some information about non-linearity and deviation of Gaussianity which could likely be present in different stage of epileptic EEGs [79]. Hence, HOS-based features become more discriminative than those of second-order measures from power spectrum. Also, unique bispectrum and bicoherernce plots have been proposed for various cardiac diseases based on heart rate [31] and phonocardiogram [70] and epilepsy using EEG signals [47], which can help to diagnose the diseases easily. Also, the HOS performs better even when the physiological signals are noisy [16,18]. This clearly shows that, the HOS is superior than the power spectral method.

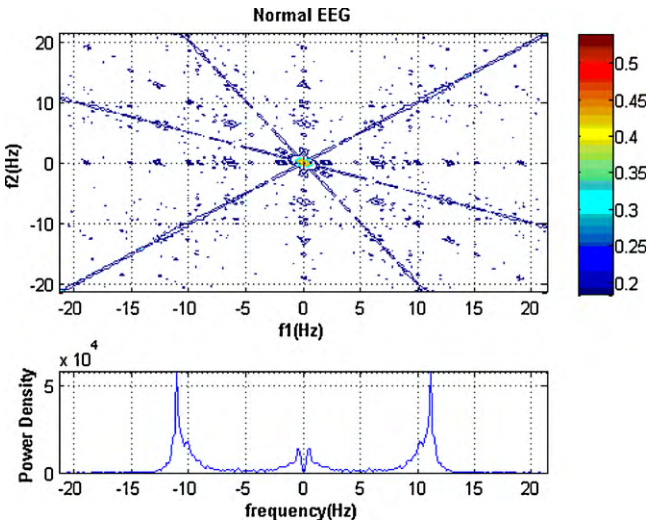

Fig. 6. Bicoherence and PSD (using Burg's method) of the normal EEG signal.

The HOS of Gaussian signals are statistically zero and the methods provide robustness to additive Gaussian noise. The 2D bispectrum and bicoherence plots of signals such as the HRV are unique for many diseases [31,57,70] and the bispectrum entropies can characterize the behaviour of physiological signals such as the HRV and the EEG [48,79]. Bispectrum based invariant features can also be used to characterized pulse shapes in physiological signals such as the ECG, EEG and 2D shapes in biomedical images [12,47,77].

Figs. 6 and 7 show the PSD (by Burg's method) and bicoherence plots of the normal EEG and normal heart rate signal. It can be seen from the figure that, HOS plot gives additional information of relationship between the different frequency components. These

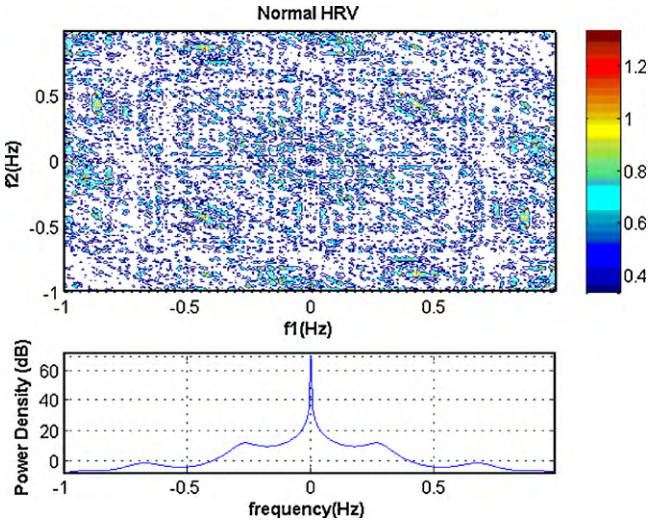

Fig. 7. Bicoherence and PSD (using Burg's method) of the normal heart rate signal.

plots can be used to discriminate different diseases [31,47,70]. And the features derived from these plots will be very useful for the identification of different classes of signals [33,57,77–79].

This review surveyed a wide range of applications of HOS in biomedical field. In some of the examples, the reasons HOS was used is also discussed giving the reader some appreciation what advantages HOS can offer as a signal processing tools. Different signal analysis tools such as Fourier transform, wavelet transform and HOS do have their own strengths and provide useful insight into the signal from different perspectives. HOS is useful in detecting nonlinear coupling, deviation from Gaussianity and features derived from it can be made invariant to shift, rotation and amplification. These features can be explored for various biomedical applications.

6. Conclusion

Physiological signals are non-stationary, non-linear and chaotic in nature. Linear and power spectral frequency methods are not very effective in the diagnosis of bio-signals. Higher order spectra (HOS) analysis has the ability to detect non-linearity, deviations from Gaussianity and the phase relationships between harmonic components. Various experiments reported that the HOS analysis (i.e. the 2D plots of bispectrum and bicoherence) of various pathological signals is unique and different HOS parameters have been used to differentiate and classify them. These features were reported to have performance superior than their power spectrum counterpart. In this paper we have discussed these HOS features and its applications on various physiological signals.

Conflict of interest

There are no conflicts of interest.

References

[1] Schetzen M. The Volterra and Wiener theories of non-linear systems. New York, NY: Wiley; 1980.
[2] Hasselman K, Munk W, MacDonald G. Bispectra of ocean waves. In: Rosenblatt M, editor. Time series analysis. New York: Wiley; 1963. p. 125–39.
[3] Chandran V, Elgar SL. Mean and variance of estimates of the bispectrum of a harmonic random process—an analysis including leakage effects. IEEE Transactions on Signal Processing 1991;39:2640–51.
[4] Chandran V, Elgar SL. Pattern recognition using invariants defined from higher order spectra—1-D inputs. IEEE Transactions on Signal Processing 1993;41:205–11.
[5] Chandran V, Elgar SL, Pezeshki C. Bispectral and trispectral characterization of transition to chaos in the duffing oscillator. International Journal of Bifurcation and Chaos 1993;3(3):551–7.
[6] El-Jaroudi A, Akgul T, Simaan M. Application of higher order spectra to multiscale deconvolution of sensor array signals. Proceeding of IEEE International Conference on Acoustics, Speech, and Signal Processing 1994;4:413–6.
[7] El-Khamy SE, Ali AF, EL-Ragal HM. Fast blind equalization using higher-order-spectra channel-estimation in the presence of severe ISI. In: Proceedings of the IEEE symposium on computers and communications. 1995. p. 248–54.
[8] Abeyratne UR, Petropulu AP, Reid JM. Higher order spectra based deconvolution of ultrasound images. IEEE Transactions on Ultrasonics, Ferroelectrics and Frequency Control 1995;42(6):1064–75.
[9] Chandran V, Carswell B, Boashash B, Elgar SL. Pattern recognition using invariants defined from higher order spectra: 2-D image inputs. IEEE Transactions on Image Processing 1997;6(5):703–12.
[10] Chandran V, Elgar SL, Nguyen A. Detection of mines in acoustic images using higher order spectral features. IEEE Journal of Oceanic Engineering 2002;27(3):610–8.
[11] Jang B, Shin C, Powers Ej, Grady WM. Machine fault detection using bicoherence spectra. In: Proceedings of the 21st IEEE Instrumentation and Measurement Technology Conference, 2004. IMTC 04, vol. 3. 2004. p. 1661–6.
[12] Ong H, Chandran V. Identification of gastroenteric viruses by electron microscopy using higher order spectral features. Journal of Clinical Virology 2005;34(3):195–206.
[13] De La Rosa JJG, Lloret I, Moreno A, Puntonet CG, Gorriz JM. Higher-order spectral characterization of termite emissions using acoustic emission probes. In: IEEE Sensors Applications Symposium SAS'07. 2007. p. 1–6.
[14] Khadra L, Al-Fahoum AS, Binajjaj S. A quantitative analysis approach for cardiac arrhythmia classification using higher order spectral techniques. IEEE Transactions on Biomedical Engineering 2005;52(11):1840–5.
[15] Muthuswamy J, Sherman D, Thakor NV. Higher order spectral analysis of EEG burst patterns during asphyxic injury. IEEE Transactions on Biomedical Engineering 1999;46(1):92–9.
[16] Nikias CL, Mendel JM. Signal processing with higher-order spectra. IEEE Signal Processing Magazine 1993;10(3):10–37.
[17] Brillinger DR, Rosenblatt M. Computation and interpretation of *k*-th order spectra. In: Harris B, editor. Spectral analysis of time series. New York: Wiley; 1967. p. 189–232.
[18] Nikias CL, Raghuveer MR. Bispectrum estimation—a digital signal processing framework. Proceedings of the IEEE 1987;75:869–91.
[19] Chandran V, Elgar SL, Vanhoff B. Statistics of tricoherence. IEEE Transactions on Signal Processing 1994;42(12):3430–40.
[20] Delorme A, Sejnowski T, Makeig S. Enhanced detection of artifacts in EEG data using higher-order statistics and independent component analysis. NeuroImage 2007;34(February (4)):1443–9.
[21] Nikias CL, Petropulu AP. Higher-order spectra analysis: a nonlinear signal processing framework. Englewood Cliffs, NJ: PTR Prentice Hall; 1993.
[22] Swami A. HOSA—Higher Order Spectra Analysis Toolbox. MATLAB CENTRAL; 2003.
[23] Elgar S, Guza RT. Statistics of bicoherence. IEEE Transactions on Acoustics, Speech and Signal Processing 1988;36(10):1667–8.
[24] Haubrich RA. Earth noises, 5 to 500 millicycles per second. Journal of Geophysical Research 1985:1415–27.
[25] Kim YC, Powers EJ. Digital bispectral analysis and its applications to nonlinear wave interactions. IEEE Transactions on Plasma Science 1979;PS-7:120–31.
[26] Elgar S, Guza RT. Statistics of bicoherence. IEEE Transactions on ASSP 1988;36(10):1667–8.
[27] Hinich MJ. Testing of Gaussianity and linearity of a stationary time series. Journal of Time Series Analysis 1982;3:169–76.
[28] Berger RD, Akselrod S, Gordon D, Cohen R. An efficient algorithm for spectral analysis of heart rate variability. IEEE Transactions on Biomedical Engineering 1986;33:900–4.
[29] Ng TT, Chang SF, Sun Q. Blind detection of photomontage using higher order statistics. In: IEEE International Symposium on Circuits and Systems (ISCAS). 2004.
[30] Zhang JW, Zheng C-X, Xie A. Bispectrum analysis of focal ischemic cerebral EEG signal using third-order recursion method. IEEE Transactions on Biomedical Engineering 2000;47(3):352–9.
[31] Chua KC, Chandran V, Acharya UR, Lim CM. Cardiac state diagnosis using higher order spectra of heart rate variability. Journal of Medical Engineering & Technology 2008;3232(2):145–55, http://www.informaworld.com/smpp/title~content=t713736867~db=all~tab=issueslist~branches=32-v.
[32] Inouye T, Shinosaki K, Sakamoto H, Toi S, Ukai S, Iyama A, et al. Quantification of EEG irregularity by use of the entropy of the power spectrum. Electroencephalography and Clinical Neurophysiology 1991;79:204–10.
[33] Zhou SM, Gan JQ, Sepulveda F. Classifying mental tasks based on features of higher-order statistics from EEG signals in brain–computer interface. Information Sciences 2008;178(6):1629–40.
[34] Witte H, Schack B, Helbig M, Putsche P, Schelenz C, Schmidt K, et al. Quantification of transient quadratic phase couplings within EEG burst patterns in sedated patients during electroencephalic burst-suppression period. Journal of Physiology (Paris) 2000;95:427–34.
[35] Witte H, Schack B, Specht M, Jäger H, Putsche P, Arnold M, et al. Interrelations between EEG frequency components in sedated intensive care patients during burst-suppression period. Neuroscience Letters 1999;260(1):53–6.
[36] Ademoglu A, Demiralp T. Quadratic phase coupling of electroencephalogram (EEG) and evoked potentials (EP). In: Proceedings of the 1992 international biomedical engineering days. 1992. p. 146–50.
[37] Schwab K, Putsche P, Eiselt M, Helbig M, Witte H. The rhythmicity of quadratic phase coupling in the trace alternant EEG in healthy neonates. Neuroscience Letters 2004;369(October (3)):179–218.
[38] Schmidt K, Witte H. Detection of quadratic phase coupling between EEG signal components by nonparametric and parametric methods of bispectral analysis. Biomedizinische Technik (Berlin) 1999;44(November (11)):314–8.
[39] Villa AEP, Tetko, IV. Cross-frequency coupling in mesiotemporal EEG recordings of epileptic patients. Journal of Physiology (Paris); in press. Corrected Proof, December 2009.
[40] Samar VJ, Swartz KP, Raghuveer MR, Braveman AL, Centola JM, Jackson JK. Quadratic phase coupling in auditory evoked potentials from healthy old subjects and subjects with Alzheimer's dementia. In: IEEE Signal Processing Workshop on Higher-Order Statistics 1993. 1993. p. 361–5.
[41] Haejeong P, Kwangsuk P. A study on the stochastic properties of the EEG using bicoherence. In: Proceedings of the 16th annual international conference of the IEEE engineering in medicine and biology society, engineering advances: new opportunities for biomedical engineers, vol. 2. 1994. p. 1314–5.
[42] Rezek I, Roberts SJ, Conradt R. Increasing the depth of anesthesia assessment. IEEE Engineering in Medicine and Biology Magazine 2007;26(2):64–73.
[43] Billard, Index bispectral de l'EEG: Bibliographie. http://www.sitanest.net/bibliographie_bis.htm [access time: 10th February 2009].
[44] Akgul T, Sun M, Sclahassi RJ, Cetin AE. Characterization of sleep spindles using higher order statistics and spectra. IEEE Transactions on Biomedical Engineering 2000;47(8):997–1009.
[45] BCI Competition II—final result. http://ida.first.fraunhofer.de/projects/bci/competition_ii/results/index.html [access time: 30th March 2009].

[46] Huang L, Sun Q, Cheng J, Huang Y. Prediction of epileptic seizures using bispectrum analysis of electroencephalograms and artificial neural network. Proceedings of the 25th annual international conference of the IEEE engineering in medicine and biology society 2003;3:2947–9.
[47] Chua KC, Chandran V, Acharya UR, Lim CM. Analysis of epileptic EEG signals using higher order spectra. Journal of Medical & Engineering Technology 2009;33(1):42–50.
[48] Chua KC, Chandran V, Acharya UR, Lim CM. Automatic identification of epileptic EEG signals using higher order spectra. International Journal of Engineering in Medicine 2009;223(4):485–95.
[49] Sabry-Rizk M, Zgallai W, El-Khafif S, Carson E, Grattan K, Thompson P. Highly accurate higher order statistics based neural network classifier of specific abnormality in electrocardiogram signals. In: Proceedings of IEEE International Conference on Acoustics, Speech, and Signal Processing 1999 (ICASSP'99), vol. 2. 1999. p. 1033–6.
[50] Patwardhan A, Moghe S, Wang K, Leonelli F. Non-linear frequency modulation and phase coupling in ECG during ventricular fibrillation. In: Proceedings of the first joint BMES/EMBS conference 1999, vol. 1. 1999. p. 307.
[51] Panoulas KI, Hadjileontiadis LJ, Panas SM. Enhancement of R-wave detection in ECG data analysis using higher-order statistics. In: Proceedings of the 23rd annual international conference of the IEEE Engineering in Medicine and Biology Society 2001, vol. 1. 2001. p. 344–7.
[52] Alliche A, Mokrani K. Higher order statistics and ECG arrhythmia classification. In: Proceedings of the 3rd IEEE International Symposium on Signal Processing and Information Technology, 2003. ISSPIT 2003. 2003. p. 641–3.
[53] Osowski S, Hoai LT, Markiewicz T. Support vector machine-based expert system for reliable heartbeat recognition. IEEE Transactions on Biomedical Engineering 2004;51(4):.582–589.
[54] Engin M. ECG beat classification using neuro-fuzzy network. Pattern Recognition Letters 2004;25(15):1715–22.
[55] MIT Arrhythmia Database. http://www.physionet.org/physiobank/database/mitdb/ [access time: 10th December 2003].
[56] Istepanian RSH, Hadjileontiadis LJ, Panas SM. ECG data compression using wavelets and higher order statistics methods. IEEE Transactions on Information Technology in Biomedicine 2001;5(2):108–15.
[57] Chua KC, Chandran V, Acharya UR, Lim CM. Cardiac health diagnosis using higher order spectra and support vector machine. Open Access Medical Informatics Journal 2009;3:1–8.
[58] Schwab K, Eiselt M, Putsche P, Helbig M, Witte H. Time-variant parametric estimation of transient quadratic phase couplings between heart rate components in healthy neonates. Journal of Medical and Biological Engineering and Computing 2006;44(12):1077–83.
[59] Bilodeau M, Cincera M, Arsenault A, Gravel D. Normality and stationarity of EMG signals of elbow flexor muscles during ramp and step isometric contractions. Journal of Electromyography and Kinesiology 1997;7(2):87–96.
[60] Zazula D. Experience with surface EMG decomposition using higher-order cumulants. Signal Processing 2001:19–24.
[61] Plevin E, Zazula D. Decomposition of surface EMG signals using non-linear LMS optimisation of higher-order cumulants. In: Proceedings of the 15th IEEE symposium on Computer-Based Medical Systems 2002. (CBMS 2002). 2002. p. 149–54.
[62] Shahid S, Walker J, Lyons GM, Byrne CA, Nene AV. Application of higher order statistics techniques to EMG signals to characterize the motor unit action potential. IEEE Transactions on Biomedical Engineering 2005;52(7):1195–209.
[63] Kaplanis PA, Pattichis CS, Hadjileontiadis LJ, Panas SM. Bispectral analysis of surface EMG. In: Proceedings of the 10th Mediterranean electrotechnical conference, vol. II. 2000. p. 770–3.
[64] Nazarpour K, Sharafat AR, Firoozabadi SMP. Application of higher order statistics to surface electromyogram signal classification. IEEE Transactions on Biomedical Engineering 2007;54(10):1762–9.
[65] X. Chen, X. Zhu, D. Zhang. A discriminant bispectrum feature for surface electromyogram signal classification. Medical Engineering & Physics; in press. Corrected Proof, Available online 03 December 2009.
[66] Hadjileontiadis LJ, Panas SM. Adaptive reduction of heart sounds from lung sounds using fourth-order statistics. IEEE Transactions on Biomedical Engineering 1997;44(7):642–8.
[67] Hadjileontiadis LJ, Panas SM. Nonlinear analysis of musical lung sound using bicoherence index. In: Proceedings of the 19th annual international conference of IEEE/EMBS 3. 1997. p. 1126–9.
[68] Hadjileontiadis LJ, Panas SM. Discrimination of heart sounds using higher-order statistics. In: Proceedings of the 19th annual international conference of the IEEE Engineering in Medicine and Biology Society, vol. 3. 1997. p. 1138–41.
[69] Rekanos IT, Hadjileontiadis LJ. An iterative kurtosis-based technique for the detection of nonstationary bioacoustic signals. Signal Processing 2006;86(12):3787–95.
[70] Ahlström C. Processing of the phonocardiographic signal—methods for the intelligent stethoscope. Thesis No. 1253. Linköping Studies in Science and Technology, Linköping; May 2006.
[71] Meste O. Bispectral reconstruction using incomplete phase knowledge: a neuroelectric signal estimation application. International Conference on Acoustics, Speech, and Signal Processing (ICASSP-97), vol. III. p. 1913–1916.
[72] Gurcan MN, Yardimci Y, Cetin AE, Ansari R. Detection of microcalcifications in mammograms using higher order statistics. IEEE Signal Processing Letters 1997;4(8):213–6.
[73] Abeyratne UR, Petropulu AP. Higher-order statistics for tissue characterization from ultrasound images. In: Proceedings of the IEEE Signal Processing Workshop on Higher-Order Statistics. 1997. p. 72–6.
[74] Balan AN, Azimi-Sadjadi M. Detection and classification of buried dielectric anomalies by means of the bispectrum method and neural networks. IEEE Transactions on Instrumentation and Measurement 1995;44(6):998–1002.
[75] Shao Y, Celenk M. Higher-order spectra (HOS) invariants for shape recognition. Pattern Recognition 2001;34(11):2097–113.
[76] Luo Y, Celenk M, Bejai P. Discrimination of malignant lymphomas and leukemia using Radon transform based-higher order spectra. Progress in Biomedical Optics and Imaging 2006;7(3).
[77] Acharya UR, Chua KC, Ng EYK, Wei W, Chee C. Application of higher order spectra for the identification of diabetes retinopathy stages. Journal of Medical Systems 2008;32(6):481–90.
[78] Chua KC, Chandran V, Acharya UR, Ng EYK, Chee C, Gupta M, Lim CM, Melissa TYJ, Gracielynne F, Suri JS. Computer-based detection of diabetes maculopathy stages using higher order spectra. In: Acharya, et al., editors. Image modeling of human eye. Artech House; 2007.
[79] Chua KC, Chandran V, Acharya UR, Lim CM. Application of higher order spectra to identify epileptic EEG. Journal of Medical Systems; in press.